Odor Context Sensing: Dual-Dimension E-nose Analysis on Odor Substances and Dispersion States

Gang Yu[†‡], Hongyi Zhao[†§], Jia-Wei Yang[†], Keyang Tang[†], and Qi Lu[*†]
[†]The Future Laboratory, Tsinghua University, Beijing, China
[‡]Academy of Arts and Design, Tsinghua University, Beijing, China
[§]The Edward S. Rogers Sr. Department of Electrical & Computer Engineering, University of Toronto, Toronto, Canada

***Abstract*—MOS-based electronic noses (e-noses) capture the temporal evolution of odor events through dynamic signals. While dispersion variations from source kinematics and environmental conditions often hinder the system performance, they offer an underexploited opportunity to infer odor context. We developed a multi-odor dataset featuring five substances (baijiu, essential oil, drain cleaner, vinegar, and coffee) across three scenarios: static open-space, passing open-space, and enclosed environments. By evaluating machine learning models for joint substance identification and dispersion-state characterization, we achieved classification accuracies of 95.5% and 81.7% respectively. These results demonstrate that e-noses can simultaneously decode chemical identity and source-environment context, enabling context-aware sensing in odor-based applications.**

***Index Terms*—Electronic Nose, Odor Classification, Odor Dispersion, Time-series Algorithm**

I. Introduction

Metal-oxide semiconductor (MOS) based electronic noses (e-noses) are widely researched for their compactness, rapid response, and cost-effectiveness [1]. MOS sensor signals are inherently shaped by the dynamic interaction between the odor source and its environment. Specifically, the spatio-temporal dispersion of chemical molecules varies substantially with the kinematic state of the source (static versus dynamic) and the environmental boundary conditions (open versus confined). These variations are fundamentally governed by the morphology of the odor plume, which emerges as airborne molecules are transported and dispersed through a combination of molecular diffusion and turbulent airflow [2], [3].

However, most e-nose studies remain restricted to controlled, static scenarios like sealed containers [4] or enclosed chambers [5], [6], leading to limited generalization in real-world settings. At the same time, the dynamic sensing capabilities of e-noses offer an underexploited potential. By producing continuous time-series data, they capture the full lifecycle of an odor event, enabling the extraction of plume-related characteristics to infer source location and motion [3], [7]. Furthermore, these patterns can decode specific 'scenarios': a sensor would distinguish the transient signal of someone walking by with a coffee cup from the steady-state signal of a coffee-filled room. This capability transforms the e-nose from a simple chemical detector into a context-aware intelligence system.

[*]Corresponding author: Qi Lu (email: luq@mail.tsinghua.edu.cn).

To address these limitations, we developed an odor dataset covering five substances (baijiu, essential oil, drain cleaner, vinegar, and coffee) across three scenarios: static open-space, passing open-space, and enclosed environments. We propose a dual-dimensional analysis framework to simultaneously identify odor substances and characterize their dispersion regimes. Evaluating both classical machine learning and neural networks, we achieved accuracies of 95.5% for dispersion-state classification and 81.7% for substance identification. These results demonstrate the feasibility of jointly decoding substance-level and source–environment–level dispersion information from standard MOS-based e-nose systems, thereby expanding the dimensionality and contextual richness of e-nose signal interpretation.

II. Materials and Methods

A. Data Collection

The e-nose system employed in this study features a self-developed sensor array of four MOS gas sensors (detailed information reported in [4]). This array was directly exposed to the ambient gas environment. The sampling frequency was fixed at approximately 37 Hz to ensure high-fidelity acquisition of transient chemical signals.

Three experimental conditions were designed to simulate varying dispersion states. Each condition was further subdivided based on certain parameters to increase the diversity of the dataset. In the first **static odor sources dispersing in open spaces** condition, the odor source was positioned stationary directly beneath the e-nose at vertical distances of 10 cm and 30 cm. This reflects the most prevalent odor scenario: fixed sniffing scenarios. The second condition, **odor sources passing in open spaces**, repesenting those odor plumes generated by a passing source such as a walking person holding a bunch of flowers. The odorant was placed on a moving belt and translated beneath the e-nose at two velocities: 0.11 m/s and 0.25 m/s. The third condition addressed **odor dispersion within confined spaces**, utilizing an 85-liter enclosure made of polypropylene (PP) material. This represents an odor uniformly diffused throughout a space, such as ambient fragrances or the aroma of a coffee shop. After a 2-minute period to allow for odor vaporing, the e-nose was introduced into the chamber under two sub-conditions: one where the source remained present, and the other where the source was removed. The experimental setup for these three diffusion states is illustrated in Figure 1.

We selected five common household odorants, including baijiu, essential oil, drain cleaner, vinegar, and hot coffee. These were presented in everyday containers to replicate real-world emission profiles as shown in Figure 1. Data acquisition was conducted over a continuous two-day period to account for potential environmental fluctuations. Each unique combination of odorant, dispersion condition, and sub-parameter was sampled at least five times. This protocol resulted in a dataset of 185 odor samples, 34,060 seconds and 1,264,840 data points, providing a rigorous foundation for characterizing both chemical identity and spatio-temporal dispersion states.

Fig. 1. Experimental setup for three dispersion states and five odor substances.

B. Data Modeling

The data modeling framework consists of three stages.

Data preprocessing. To filter out long-time drifting signals and high-frequency circuit noise, a band-pass filter was first applied to retain frequency components between $5e^{-5}$ Hz and 3 Hz. Subsequently, a moving-average filter (window size = 10 points, stride = 1) was used to further smooth signals. Data observations indicate that signal shape variations (not individual sensor channel responses) are more indicative of dispersion states. Thus, Z-score normalization was additionally applied to each sensor channel per recording file for dispersion-state classification task, implemented unsupervised without label information.

Sliding-window segmentation. Since the amount of collected data is limited, a sliding-window strategy was adopted to augment the dataset and extract features [6], [8]. Each odor sample file was segmented using fixed-length windows of 10 seconds with a 50% overlap between adjacent windows. All windows were first detected whether the odor event happened. If the mean values across all channels exceeded the threshold (20*abs(baseline) for unnormalized data; 0.5*abs(baseline) for normalized data), the window was labeled as *odor present* and forwarded to the downstream classifiers.

Model Design and Training. The evaluation was framed as two parallel classification tasks using identical input windows: (i) odor-substance classification and (ii) dispersion-state classification. We compared manual-feature-based machine learning (Support Vector Machine, SVM) with various time-series neural networks (Multi-Layer Perceptron, MLP; 1D-Convolutional Neural Network, 1D-CNN; MiniRocket; Long Short-Term Memory, LSTM; Transformer) to analyze the temporal evolution of odor plumes. Model configurations are summarized below:

- Manual features: Time-domain (mean, standard deviation, maximum, minimum, root mean square, linear regression slope); frequency-domain (dominant frequency, spectral centroid, spectral bandwidth, spectral energy).
- MLP: Adam optimizer, tanh activation, two hidden layers (256 neurons each), 1000 max iterations, softmax output layer.
- MiniRocket: Default sktime hyperparameters (10,000 convolution kernels, 32 max dilations per kernel, full reference length).
- 1D-CNN: Conv1d-1 (in=4, out=32, kernel=7, padding=3) - BatchNorm1d - ReLU - Conv1d-2 (in=32, out=64, kernel=5, padding=2) - BatchNorm1d - ReLU - Conv1d-3 (in=64, out=64, kernel=3, dilation=2, padding=2) - BatchNorm1d - ReLU - 1D Average Pooling - Linear(64-64) - ReLU - Dropout(0.3) - Linear(64-target classes). Adam optimizer, CrossEntropy loss.
- LSTM: Bidirectional LSTM (2 layers, hidden size=128, dropout=0.3) - Linear(256-128) - ReLU - Dropout(0.3) - Linear(128-target classes). Adam optimizer, CrossEntropy loss.
- Transformer: Input projection (4-64) - Sin-Cosine positional encoding - Transformer Encoder (4 layers, 4 heads, dim feedforward=128, dropout=0.2) - 1D Average Pooling - Linear(64-128) - ReLU - Dropout(0.3) - Linear(128-target classes). AdamW optimizer, CrossEntropy loss.

To avoid window-overlap induced information leakage, data was split at the file level instead of window level. For each odor and dispersion condition, two full sample files were randomly allocated to the test set ($\sim$20%), with the rest for training, ensuring no test segments overlapped with the training set. 20 times of random data splitting, model training and testing were conducted, and the average performances were obtained.

III. Results and Discussion

A. Data visualization

Figure 2 illustrates the distinct signal morphologies under the three dispersion states, which remain consistent across odorants.

Dispersion Signatures: The *fixed* state is characterized by stochastic fluctuations reflecting turbulent odor plumes. In contrast, the *passing-by* state generates a singular, transient peak due to brief exposure. The *space* state produces a sustained plateau; the presence of an odor source introduces slight fluctuations, whereas a removed source results in a stabilized baseline.

Odorant Fingerprints: While dispersion governs the signal's temporal envelope, the chemical identity is encoded in the sensor-specific response magnitudes. For instance, the sensor array exhibits a distinct preference for essential oil on channel S3, whereas S4 shows a dominant response to coffee.

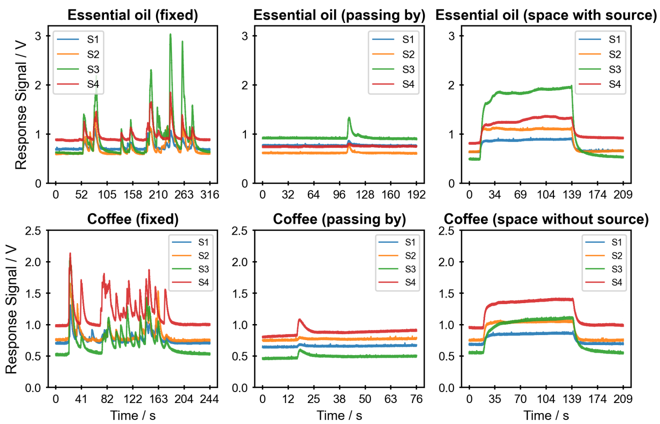

Fig. 2. Original signals of different dispersion states and odor substances.

B. Classification

TABLE I
CLASSIFICATION RESULTS

Model	Classification Task			
	Odor substance		Dispersion state	
	Accuracy	F1 score	Accuracy	F1 score
Manual-SVM	62.4(±10.2)	60.9(±10.8)	73.6(±1.9)	68.8(±2.3)
MLP	**81.7(±7.9)**	79.1(±9.0)	83.5(±2.0)	79.1(±2.3)
MiniRocket -SVM	65.8(±9.0)	64.2(±10.1)	95.3(±1.7)	94.0(±2.3)
1D-CNN	79.6(±7.8)	78.4(±8.0)	**95.5(±1.2)**	**94.4(±1.6)**
LSTM	79.4(±6.3)	77.3(±7.4)	73.7(±1.3)	70.5(±1.2)
Transformer	80.9(±6.6)	**79.4(±7.7)**	91.5(±1.8)	89.1(±2.5)

Table I presents the performance of the evaluated models on the two classification tasks. The results show that time-series–based models such as MiniRocket, 1D-CNN and Transformer outperform the manual feature–engineering approach significantly. This performance gap suggests that traditional hand-crafted features are insufficient for capturing the high-dimensional, non-linear fluctuations inherent in dynamic odor dispersion.

Specifically, 1D-CNN outperformed other models in dispersion-state classification, achieving a peak accuracy of 95.5% and an F1 score of 94.4%. This highlights the effectiveness of convolutional filters in capturing representative temporal patterns within the dynamic gas signals. For the more challenging task of odorant identification, MLP and Transformer demonstrated superior results, with accuracies of 81.7% and 80.9%, respectively. Notably, while MiniRocket and 1D-CNN showed competitive results in dispersion classification, their performance dropped significantly in substance identification, indicating that simple kernel-based transforms may struggle to resolve the subtle chemical variations between different odorants.

A significant finding of these results is that MOS-based e-noses can simultaneously extract chemical identity and environmental context. The high accuracy in dispersion classification (up to 95.5%) demonstrates that the sensor fluctuations caused by environmental turbulence actually contains structured information. This opens the door for context-aware gas sensing, where a system can first identify the dispersion state to calibrate its substance recognition logic, thereby improving generalization in open-field e-nose applications.

IV. CONCLUSION

This study introduces a multi-odor dataset encompassing five representative substances (baijiu, essential oil, drain cleaner, vinegar, and coffee) across three typical dispersion scenarios: static open-space, passing open-space, and enclosed environments. By evaluating diverse machine learning and time-series neural networks, we achieved accuracies of 95.5% for dispersion-state classification and 81.7% for odorant identification.

These results signify a paradigm shift in gas sensing: MOS-based e-noses are no longer mere chemical detectors, but intelligent perception systems capable of parsing complex odor scenes. By integrating chemical identity with environmental context, these systems can now decode odor events more comprehensively, such as distinguishing between static ambient aromas and transient human-driven activities. This high-level contextual awareness provides a foundation for future olfactory agents to execute precise, context-specific actions.

ACKNOWLEDGMENT

This work was supported in part by the Foundation of National Key Laboratory of Human Factors Engineering, Grant NO. HFNKL2023J08, in part by the National Natural Science Foundation of China, Grant No. 62441219 and Grant No. 62172252, and in part by the National Key R&D Program of China, Grant No. 2024YFC3810602.

REFERENCES

[1] J. Li, E. Na, X. Liang, Q. Liang, M. Fan, H. Chen, G.-D. Li, and X. Zou, "Surface oxygen chemistry of metal oxide semiconductors for gas-sensing applications," *Inorganic Chemistry Frontiers*, vol. 11, pp. 8602–8626, 2024.

[2] J. Murlis, J. S. Elkinton, R. T. Carde *et al.*, "Odor plumes and how insects use them," *Annual review of entomology*, vol. 37, no. 1, pp. 505–532, 1992.

[3] T. Nakamoto and H. Ishida, "Chemical sensing in spatial/temporal domains," *Chemical reviews*, vol. 108, no. 2, pp. 680–704, 2008.

[4] Y. Sun, G. Yu, Q. Lu, H. Han, J.-W. Yang, and Y. Xu, "An electronic nose device with rapid and universal odor detection capability," *Sensors and Actuators B: Chemical*, p. 137871, 2025.

[5] W. Ni, T. Wang, Y. Wu, L. Chen, M. Zeng, J. Yang, N. Hu, B. Zhang, F. Xuan, and Z. Yang, "Robust odor detection in electronic nose using transfer-learning powered scentformer model," *ACS sensors*, vol. 10, no. 5, pp. 3704–3712, 2025.

[6] D. Feng, C. Li, W. Dai, and P. P. Liang, "Smellnet: A large-scale dataset for real-world smell recognition," *arXiv preprint arXiv:2506.00239*, 2025.

[7] T. Nakamoto, H. Ishida, and T. Moriizumi, "Peer reviewed: A sensing system for odor plumes." *Analytical chemistry*, vol. 71, no. 15, pp. 531A–537A, 1999.

[8] N. M. Norwawi, "Sliding window time series forecasting with multilayer perceptron and multiregression of covid-19 outbreak in malaysia," in *Data Science for COVID-19*. Elsevier, 2021, pp. 547–564.